Compact first and second order polarization mode dispersion emulator

Yang Zhang (张 阳), Shiguang Li (李世光), and Changxi Yang (杨昌喜)

State Key Laboratory of Precision Measurement Technology and Instruments, Department of Precision Instrument, Tsinghua University, Beijing 100084

Received December 30, 2004

We propose a 1st and 2nd order polarization mode dispersion emulator (PMDE) with one variable differential group delay (DGD) element using birefringence crystals and four polarization controllers (PCs). Monte Carlo simulations demonstrate that the output 1st and 2nd order polarization mode dispersion (PMD) generated by the PMDE consists with statistic theory. Compared with former PMDEs, this design is tunable, lower-cost, and more integrated for fabrication, which shows response time of 150 μs, response frequency of 3.8 kHz, working wavelength of 1550 nm, total power consumption of less than 3 W, working range of 0—84 ps and 0—3600 ps^2 for 1st and 2nd order PMD emulation, respectively. Also, it is programmable and can be controlled by either singlechip or computer. It can be applied to study the outage probability of optical communication systems due to PMD effect and the effectiveness of PMD compensation.

OCIS codes: 060.2330, 060.2420.

Polarization mode dispersion (PMD) is becoming major system impairment in high speed and long distance optical fiber transmission systems. Since the PMD-induced pulse spreading is a frequency-dependent statistic parameter and varies randomly over time, it is difficult to be compensated[1−3]. Large length of single mode optical fiber is needed to generate certain amount of PMD in laboratory, and the PMD effect in the fiber varies slightly and slowly over time. Therefore, PMD emulators (PMDEs) have been attracting great research interest, which can be applied to study the outage probability of systems due to PMD effect and the effectiveness of PMD compensation. PMDEs are typically based on concatenation of several segments of polarization maintaining fibers (PMFs) or birefringent crystals via rotatable fiber connectors (FCs) or polarization controllers (PCs). More than 15 segments are required to generate the statistic distributions of PMD parameters that resemble the presence in real optical communication fibers when the PMF-FC model is used[4]. Moreover, a relatively long length of PMF is needed to generate certain amount of differential group delay (DGD) since it has smaller birefringence compared with birefringent crystals. This causes harmful nonlinear optical effects for the transmission systems. Furthermore, it has been pointed out that fewer segments will be required and the output PMD will approach what is in real fibers more precisely if the PCs are used to concatenate the segments instead of the FCs[5].

Various techniques for PMD emulation have been reported, among which are a PMDE with 12 segments of PMFs proposed by Waddy *et al.*[6] and another with 3 programmable DGD elements proposed by Yan *et al.*[7]. However, few of these have been fabricated and commercialized because of high complexity and cost. In this letter, we focus on combining advantages of different designs and reducing the complexity and cost of the device while maintaining satisfying performance.

We simplify the PMDE into only one compact variable DGD element and 4 PCs, as shown in Fig. 1. The variable DGD element is based on concatenations via six magneto-optic polarization rotators of six birefringence crystals whose lengths decrease in a binary power series. Compared with former PMDE schemes, this PMDE is compact, tunable, lower-cost, and more integrated for fabrication while maintaining satisfying performance. It shows response time of 150 μs, response frequency of 3.8 kHz, working wavelength of 1550 nm, total power consumption of less than 3 W, working range of 0—84 ps and 0—3600 ps^2 for 1st and 2nd order PMD emulation, respectively. Also, it is programmable and can be controlled by either singlechip or computer.

In order to demonstrate the performance of this PMDE, we discuss the model composed of 4 PCs and 4 fixed DGD elements as shown in Fig. 2, where ω is the angular carrier frequency of the light, C_i is the rotation matrix of the ith PC, $\vec{\tau_i}$ is the 1st order PMD vector of the ith DGD element whose orientation is set to be parallel to the s_1 axis of the Stokes space, and R_i is the Muller matrix of the ith DGD element. Using the concatenation rules, one can get

$$\begin{cases} \vec{\tau}^{(i)} = \vec{\tau_i} + R_i C_i \vec{\tau}^{(i-1)} \\ \vec{\tau_\omega}^{(i)} = \vec{\tau_i} \times (R_i C_i \vec{\tau}^{(i-1)}) + R_i C_i \vec{\tau_\omega}^{(i-1)} \end{cases}, \quad (1)$$

where $\vec{\tau}^{(i)}$ and $\vec{\tau_\omega}^{(i)}$ are the output 1st and 2nd order PMD vectors of the ith segment, and the input $\vec{\tau}^{(0)}$

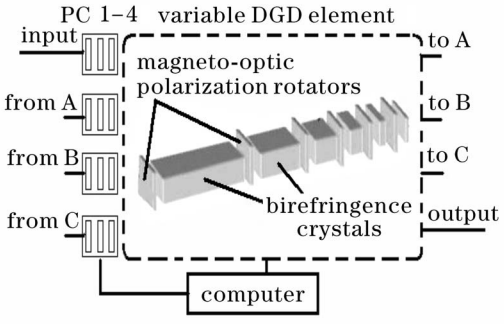

Fig. 1. Compact 1st and 2nd order PMDE.

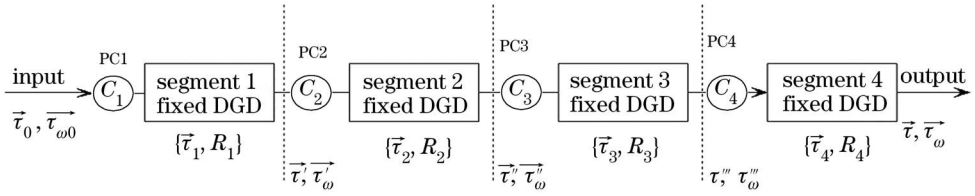

Fig. 2. Block diagram of the 4-segment model.

and $\overrightarrow{\tau_\omega}^{(0)}$ are assumed to be zero.

Each of the PCs is composed of 3 tunable phase shifters (TPSs) with sequently 45°-horizontal-45° linearly polarized birefringence axes in physical space. The rotation axes of their rotation matrices are along s_2-s_1-s_2 directions, respectively. Therefore, we have

$$C_i = T_2(\theta_{i3})T_1(\theta_{i2})T_2(\theta_{i1}), \quad (i = 1, 2, 3, 4), \tag{2}$$

where T_1 and T_2 represent the rotation matrices whose axes are along s_1 and s_2, respectively, and θ_{ij} represents the rotation angle of the jth TPS of the ith PC.

Monte-Carlo simulations are carried out to study the effectiveness of this model. Rotation angles of the TPSs are randomized to be uniformly distributed between $[0, 2\pi]$, while $|\overrightarrow{\tau_i'}| = 10$ ps $(i = 1, 2, 3, 4)$, $\lambda = 1550$ nm. Based on 100,000 statistically independent samples, the probability densities of the output 1st and 2nd order PMD $|\tau|$ and $|\tau_\omega|$ are illustrated in Fig. 3, while the theoretic distributions are designated by PMD statistical theory[8]

$$p_{|\overrightarrow{\tau}|}(x) = \frac{8}{\pi^2\tau_{\rm m}}\left(\frac{2x}{\tau_{\rm m}}\right)\exp\left[-\frac{(2x/\tau_{\rm m})^2}{\pi}\right], \quad x \geq 0 \quad \text{(Maxwellian)}, \tag{3}$$

$$p_{|\overrightarrow{\tau_\omega}|}(x) = \frac{8}{\pi\tau_{\rm m}^2}\frac{4x}{\tau_{\rm m}^2}\tanh(4x/\tau_{\rm m}^2)\,\mathrm{sech}(4x/\tau_{\rm m}^2), \quad x \geq 0, \tag{4}$$

where $\tau_{\rm m}$ represents the mean DGD of the PMDE.

The simulation results show that the probability densities of $|\tau|$ and $|\tau_\omega|$ suit the PMD statistic theory well. We use the deviation of the emulated PMD from the ideal probability density function (PDF) as a meteyard, which is defined by $\sigma = \sum_i |p_{\rm emul}(x_i) - p_{\rm ideal}(x_i)|^2$, where $p_{\rm emul}(x_i)$ and $p_{\rm ideal}(x_i)$ are the probability densities of the emulated and ideal PMDs, respectively. For the simulation results above, σ of the 1st and 2nd order PMD are $\sigma_1 = 4.00 \times 10^{-4}$ and $\sigma_2 = 5.32 \times 10^{-4}$, respectively, while for a 12-segment PMDE using PMFs and FCs, $\sigma_1 = 1.08 \times 10^{-4}$, $\sigma_2 = 2.3 \times 10^{-3}$, and for theoretic PMD model as a concatenation of 1200 randomly oriented, linearly birefringent fiber sections of about 100-beat lengths each, $\sigma_1 = 3.14 \times 10^{-5}$, $\sigma_2 = 2.74 \times 10^{-7}$.

If the number of the PC-DGD segments is reduced to 3, the simulation results do not suit the PMD statistic theory (Fig. 4(a)), because the quantity of random parameters (or total degree of freedom (DOF)) is not large enough. On the other hand, using more PC-DGD segments only slightly improves the performance of the PMDE. If the TPSs that compose each PC are reduced to 2, the simulation results do not suit the PMD statistic theory (Fig. 4(b)). This is because 2 DOFs cannot rotate at arbitrary incident state of polarization (SOP) to make the output SOPs cover the entire Poincare sphere (Fig. 4(b), 2000 samples). This conflicts with the PMD stochastic characteristic in real fibers. The output SOPs

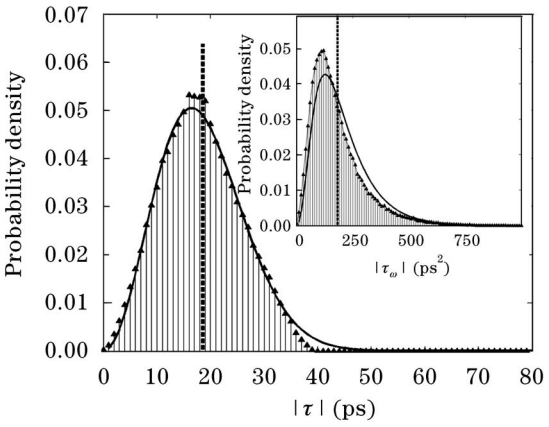

Fig. 3. Probability density of $|\tau|$ and $|\tau_\omega|$, 4 PC-DGD segments, 3 TPSs in each PC. Vertical dashed line: mean value; stem plots: simulation results; solid curve: theoretic distribution.

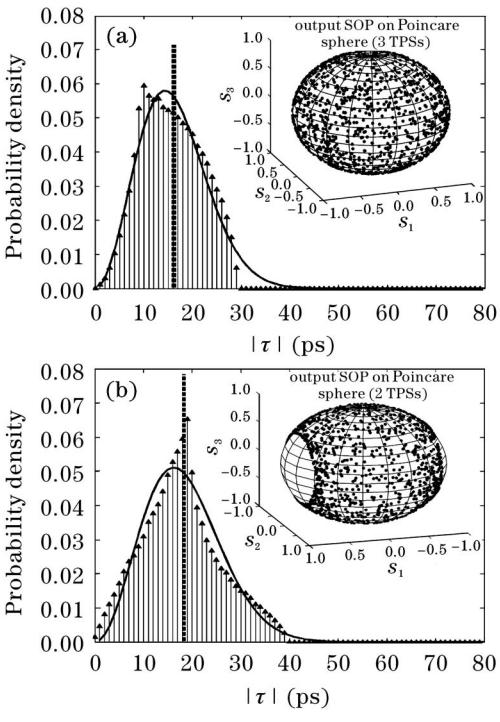

Fig. 4. Probability density of $|\tau|$ and $|\tau_\omega|$. (a) 3 PC-DGD segments, 3 TPSs in each PC; (b) 4 PC-DGD segments, 2 TPSs in each PC.

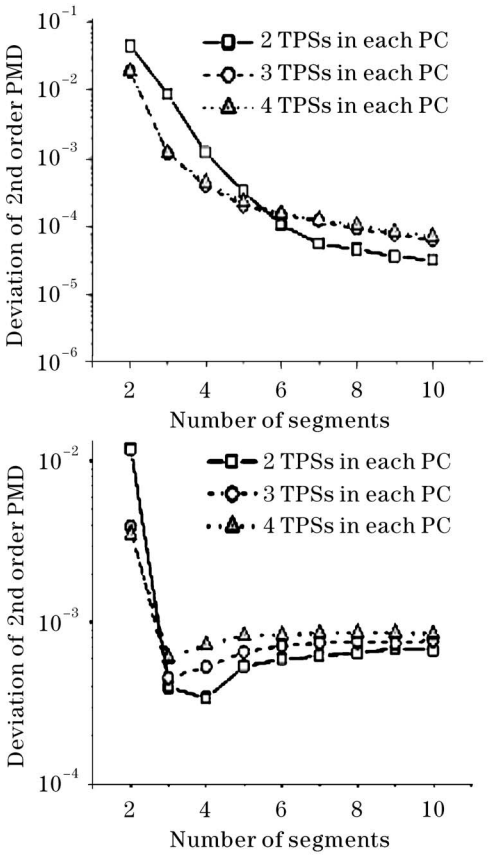

Fig. 5. Deviation of the emulated PMD from the ideal PDF.

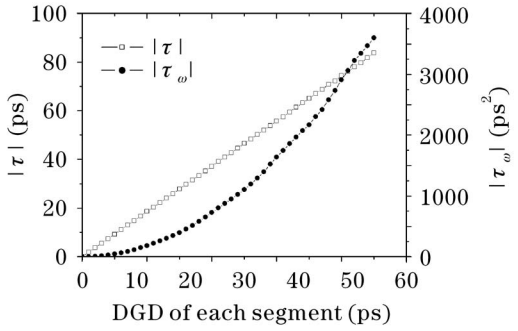

Fig. 6. $|\vec{\tau}|_{\mathrm{M}}$ and $|\vec{\tau_\omega}|_{\mathrm{M}}$ vary with DGD of each segment.

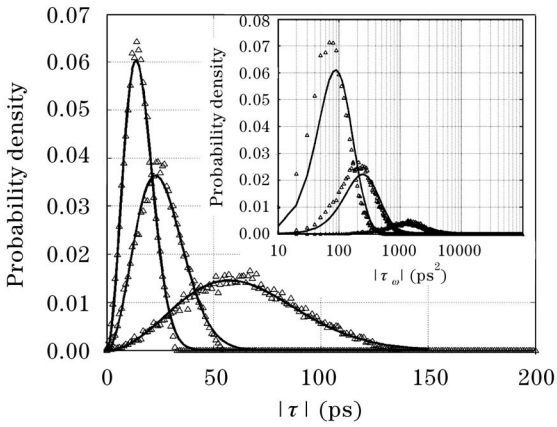

Fig. 7. Three pairs of $|\tau|$ and $|\tau_\omega|$ with different mean values.

will cover the entire Poincare sphere when at least 3 DOFs are used in each PC (Fig. 4(a), 2000 samples). Unequal DGD segments will improve the performance of the PMDE only when more than 10 segments are used. The deviations σ_1 and σ_2 versus the number of PC-DGD segments are shown in Fig. 5. Considering the complexity and cost of the device, the configuration of 4 segments and 3-DOF PCs is preferred, in which both σ_1 and σ_2 are less than 0.001.

The compact PMDE shown in Fig. 1 works the same way as the 4-segment model described above, except that variable DGD element using birefringence crystals instead of PMFs compacts the size of the device, avoids chromatic dispersion and nonlinear effects, and makes it possible for the optical signal to transmit 4 times through it. We use the variable DGD module based on concatenations via six magneto-optic polarization rotators of six birefringence crystals whose lengths decrease in a binary power series. YVO_4 crystal is recommended as the birefringent element since it shows large birefringence ($\Delta n = 0.2$) at 1550 nm, facility in machining, low insertion loss, and low cost. This variable DGD element shows insertion loss smaller than 3 dB, maximum DGD of 44.6 ps, control step of 1.4 ps, compact size, broad bandwidth, and immunity to environmental vibrations. Besides, a PC comprising three magneto-optic crystal polarization rotators and two non-rotatable quarter wave plates in between can be used instead of the PC composed of three TPSs since it also has DOF of 3 while providing compact size and low cost.

Controlling the DGD value of the variable DGD element between 0—44.6 ps by a singlechip or a computer program, the PMDE generates 1st order PMD with mean DGD $|\tau|_{\mathrm{M}}$ of 0—84 ps and the corresponding 2nd order PMD with mean value $|\tau_\omega|_{\mathrm{M}}$ of 0—3600 ps^2, as shown in Fig. 6. Figure 7 represents 3 pairs of $|\tau|$ and $|\tau_\omega|$ while $|\tau|_{\mathrm{M}} = 15.32, 25.75, 64.47$ ps and $|\tau_\omega|_{\mathrm{M}} = 125.92, 342.27, 2181.70$ ps^2, respectively.

In conclusion, a 1st and 2nd order PMDE with one variable DGD element using birefringent crystals and 4 polarization controllers is proposed. Compared with former PMDE schemes, this PMDE avoids harmful chromatic dispersion and nonlinear effects, and it is compact, tunable, lower-cost, and more integrated for fabrication while maintaining satisfying performance. It shows response time of 150 μs, response frequency of 3.8 kHz, working wavelength of 1550 nm, total power consumption less than 3 W, working range of 0—84 ps and 0—3600 ps^2 for 1st and 2nd order PMD emulation, respectively. Also, it is programmable and can be controlled by either singlechip or computer. Numerical simulation shows that the probability densities of the magnitudes of output 1st and 2nd order PMD vectors generated by the PMDE suit the PMD statistic theory well. This PMDE can be applied in the research of the tolerance of optical transmission systems to the PMD effect and the effectiveness of PMD compensators.

This work was in part supported by the Trans-Century Training Programme Foundation for the Talents by the

Ministry of Education of China. Y. Zhang's e-mail address is zhangyang99@mails.tsinghua.edu.cn.

References

1. R. Noé, D. Sandel, and V. Mirvoda, IEEE J. Sel. Top. Quantum Electron. **10,** 341 (2004).
2. L. Xi, X. Zhang, L. Yu, G. Zhou, H. Zhang, N. Zhang, J. Zhang, B. Wu, T. Yuan, M. Yao, and B. Yang, Chin. Opt. Lett. **2,** 262 (2004).
3. T. Li, M. Wang, Y. Shi, J. Cui, and S. Jian, Chin. J. Lasers (in Chinese) **30,** 518 (2003).
4. R. Khosravani, I. T. Lima, P. Ebrahimi, E. Ibragimov, A. E. Willner, and C. R. Menyuk, IEEE Photon. Technol. Lett. **13,** 127 (2001).
5. I. T. Lima, R. Khosravani, P. Ebrahimi, E. Ibragimov, C. R. Menyuk, and A. E. Willner, J. Lightwave Technol. **19,** 1872 (2001).
6. D. S. Waddy, L. Chen, and X. Bao, IEEE Photon. Technol. Lett. **15,** 534 (2003).
7. L. Yan, M. C. Hauer, Y. Shi, X. S. Yao, P. Ebrahimi, Y. Wang, A. E. Willner, and W. L. Kath, J. Lightwave Technol. **22,** 1051 (2004).
8. J. Cai, M. Xu, and X. L. Yang, Acta Opt. Sin. (in Chinese) **23,** 170 (2003).